Proceedings of the 16th IKM 2003, Gürlebeck, Hempel & Könke (eds.), Weimar, Germany, June 10-12, 2003, ISSN 1611-4086

Application of the "Fictitious Crack Model" to meshless crack growth simulations

Thomas Most & Christian Bucher
Institute of Structural Mechanics, Bauhaus-University Weimar, Marienstrasse 15, D-99423 Weimar, Germany

1 Introduction

By applying the classical Finite Element Method to discrete crack propagation simulations a very frequent adaptive remeshing is necessary. This requires a consistent transformation of the state variables. By using finite elements the stress distribution is discontinuous along the element edges, which complicates this transformation. In the last years meshless simulation methods have been developed where a continuous stress distribution can be reproduced. This enables a much easier transformation of state variables. A different method to model discontinuities is the Extended Finite Element Method (Moës et al. 1999) which is not used in this study.
In this paper a meshless component is presented, which internally uses the common meshless interpolation technique "Moving Least Squares" (Lancaster and Salkauskas 1981), (Belytschko et al. 1994). In contrast to usual meshless integration schemes like the cell quadrature and the nodal integration in this study integration zones with triangular geometry spanned by three nodes are used for 2D analysis. The boundary of the structure is defined by boundary nodes, which are similar to finite element nodes. By using the neighborhood relations of the integration zones an efficient search algorithm to detected the nodes in the influence of the integration points was developed. The components are directly coupled with finite elements by using a penalty method (Häussler-Combe 2001).
An widely accepted model to describe the fracture behavior of concrete is the "Fictitious Crack Model" (Hillerborg et al. 1976) which is applied in this study, which differentiates between micro cracks and macro cracks, with and without force transmission over the crack surface, respectively. This model has been already applied in some meshless algorithms (Häussler-Combe 2001),(Cichón and Jaśkowiec 1999),(Carpinteri et al. 2001). In these studies the crack surface is modeled as an internal polygon. The crack surface forces are reproduced by using integration zones with internal discontinuities (Häussler-Combe 2001) or special surface nodes at the crack tip (Carpinteri et al. 2001). In this study the crack surface is discretized by node pairs in form of a polygon, which is part of the boundary. To apply the "Fictitious Crack Model" finite interface elements are included between the crack surface nodes. The determination of the maximum principal strain at the crack tip is done following Häussler-Combe 2001 by introducing an influence area around the singularity.
The presented algorithms had been implemented in the SLang Software package (Bucher et al. 2002), which is available at the Bauhaus-University for research activities. With this package the presented numerical example has been calculated.

2 Mechanical formulation

2.1 Meshless interpolation

In this section only a brief overview of the the "Moving Least Squares" approximation (Lancaster and Salkauskas 1981, Belytschko et al. 1994) is given because this approximation type was applied in a number of studies (e.g. Belytschko et al. 1995a, Belytschko et al. 1995b).
To interpolate an arbitrary function by using a polynomial we get

$$u(\mathbf{x}) = \begin{pmatrix} 1 & x & y & x^2 & ... \end{pmatrix} \begin{bmatrix} a_1 \\ : \\ a_n \end{bmatrix} = \mathbf{p}^T(\mathbf{x})\mathbf{a}, \tag{1}$$

with the base vector $\mathbf{p}(\mathbf{x})$ and the coefficient vector $\mathbf{a}$. If the number of interpolation points m is equal to the number of coefficients n the problem can be solved directly like in the Finite Element Method and the coefficients can be given as

$$\mathbf{a} = \mathbf{P}^{T^{-1}}\mathbf{u}; \quad \mathbf{P} = (\mathbf{p}_1 ... \mathbf{p}_m). \tag{2}$$

By using the MLS-approximation, where $m > n$, the system of equations is overdetermined. To solved this optimization problem by minimizing the least squares error we obtain the following formulation

$$\mathbf{Pu} = \mathbf{PP}^T\mathbf{a}. \tag{3}$$

To represent the influence of distances between the interpolation points, e.g. to model geometrical discontinuities, a weighting function is used in the least square approach which leads to

$$u(\mathbf{x}) = \mathbf{\Phi}^{mls}\mathbf{u}, \quad \mathbf{\Phi}^{mls} = \mathbf{p}^T\mathbf{A}(\mathbf{x})^{-1}\mathbf{B}(\mathbf{x}), \tag{4}$$

with

$$\begin{aligned} \mathbf{B}(\mathbf{x}) &= \mathbf{PW}(\mathbf{x}), \\ \mathbf{A}(\mathbf{x}) &= \mathbf{PW}(\mathbf{x})\mathbf{P}^T, \\ \mathbf{W}(\mathbf{x}) &= diag(w(d_1), ..., w(d_m)). \end{aligned} \tag{5}$$

The weighting function $w(d_m)$, formulated depending on the distance d, can be chosen as (Häussler-Combe 2001)

$$w(d) = \begin{cases} w_g(d) & d \leq D \\ 0 & d > D \end{cases}, \quad w_g(d) = e^{-\left(\frac{d}{\alpha D}\right)^2}, \tag{6}$$

where D is the influence radius. By choosing the base polynomial $\mathbf{p}$ linear with $n = 3$ the MLS-approximation can reproduce every linear function exactly. Functions of higher order will not be interpolated exactly, but will be optimally approximated. In contrast to the finite element interpolation, then the interpolating function does not pass through the nodal values

$$\mathbf{\Phi}_i^{mls}(\mathbf{x}_j) \neq \boldsymbol{\delta}_{ij}. \tag{7}$$

which leads to problems in fulfilling the boundary conditions. Different possibilities to solve this problem, like the application of Lagrange multipliers (Belytschko et al. 1994), the introduction of a penalty term (Häussler-Combe 2001) and the usage of special boundary components (Karutz 2000),

have been developed in the recent years. By using Lagrange multipliers, the system of equations, which has to be solved, becomes larger and special solvers are required due to the singularity of the coefficient matrix. The penalty solution can force fulfillment of the boundary conditions, but the correct choice of the penalty term is difficult. The formulation of boundary components fulfills the boundary conditions but is very un-practical for the coupling with finite elements. To enable a direct coupling, which is necessary for a simple transformation of finite elements into meshless components and the uncomplicated application of random fields, in this study the penalty method is preferred.

2.2 Integration, boundary discretization and search algorithm

Common integration schemes in MLS-based meshless methods are the integration via a cell quadratures (Belytschko et al. 1996), which is a kind of a structure-independent background mesh, the element quadrature (Belytschko et al. 1996), in which the background mesh is coupled to the structure, and the nodal integration (Beissel and Belytschko 1996), in which no background mesh is necessary. In the first two methods the necessary integration order is uncertain. This is caused be the fact, that the node distribution, which develops during the simulation, may not be identical in each cell and may reach a critical value. By the nodal integration the main problem is the much higher numerical effort. By all methods, the integration across lines of discontinuity needs special attention, because crack geometries and structure surfaces do not necessarily coincide with the cell or nodal influence boundaries.
For these reasons a different integration scheme was used. In the presented 2D analysis this method uses integration zones with triangular geometry spanned by three nodes. The boundary of the structure is defined by boundary nodes, which enables the direct coupling with finite elements. The crack surfaces are discretized by node pairs as parts of the boundary. To compute the integration zones the Advancing Front Method (Peraire et al. 1987) with a modification to consider arbitrary external and internal boundaries is used. In crack growth simulations the integration zones have to be adapted only around the moving crack tips. An exemplary node distribution with belonging triangle zones is shown in Fig.1.
The determination of these nodes, which are located in the influence radius of an integration point, can be sped up by using the neighborhood relations of the presented triangular integration zones. This necessitates the storage of the determined node incidences during the computation of the triangles. For a given integration point the search algorithm detects these triangles, which are neighbors of first and second order of the triangle, which this integration point is part of. All nodes, which span these neighbor triangles are called neighbor nodes. Then only the neighbor nodes have to be checked for their distance to the integration point. This is illustrated exemplarily in Fig.2.

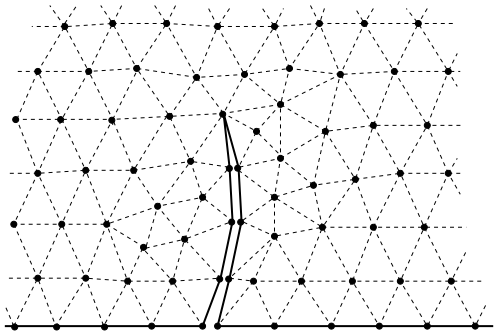

Figure 1: Boundary discretization and integration zones at a crack tip

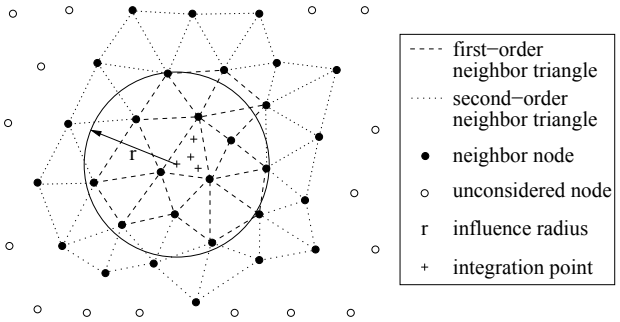

Figure 2: Improved influencing node determination by using neighborhood relations

The computational effort to determine the influencing nodes of one integration point is for larger sys-

tems independent of the total node number. The total numerical cost of the search procedure depends almost linearly on the total number of integration points. By investigating all nodes for every integration points the numerical effort is nearly proportional to the product of the node number and the integration point number, which shows the efficiency of the presented improved algorithm.

2.3 Crack modeling

In this study the crack growth behavior of concrete is in the point of interest. Therefore the classical linear fracture hypotheses (Gross 1996), which were mainly developed for metals, are not applied. A widely accepted crack model for concrete is the "Fictitious Crack Model" (Hillerborg et al. 1976) where a force transmission across the crack surface is introduced for micro cracks. For macro cracks no forces will be transmitted. If the maximum principal tensile strain exceeds a material specific ultimate strain, a micro crack will arise. The macro crack develops from a micro crack, if a critical crack width is reached. If the ultimate strain at a crack tip is exceeded the crack keeps on growing. In order to remove the local influence of singularities at the crack tip the strains values will be computed by introducing an influence area around the singularity like shown in Fig.3 (Häussler-Combe 2001). The comparative strain value $\bar{\boldsymbol{\epsilon}}$ is calculated from the strain values in the influence area as

$$\bar{\boldsymbol{\epsilon}} = \int_{\Omega_t} w(|\mathbf{x} - \mathbf{x}_t|) \cdot \boldsymbol{\epsilon}(\mathbf{x}) d\Omega, \tag{8}$$

where $\mathbf{x}_t$ is the position of the crack tip, Ω_t is the influence area and $w(d)$ is a weighting function, which can be chosen similar to the MLS-weighting function in Eq.(6). The size of the influence radius can be determined by the numerical adjustment of experimental data (Häussler-Combe 2001).
After the calculation of the direction and the length of the new crack increment, the node discretization and the integration zones around the crack tip have to be adapted. For this purpose the area of these triangles through which the new crack increment passes and their neighbors will be triangulated again by duplicating the node at the previous crack tip. To improve the geometry of the new triangles the Laplace smoothing algorithm (Herrmann 1976) is applied to modify the positions of the nodes, which are not members of the crack surface and the determined local boundary. In Fig. 4 the local adaptation around the new crack increment is shown exemplarily. After this triangulation the integration point data have to be transformed from the old positions to the new one, which is done directly by using the MLS-approximation. For a detailed description of the random field data transformation the reader is referred to Most and Bucher 2003.

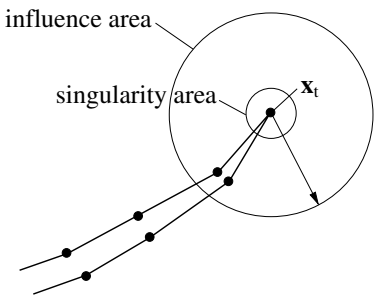

Figure 3: Determination of a comparative strain value by introducing an influence area

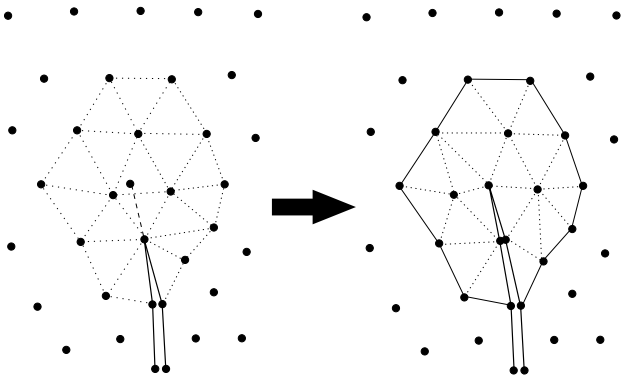

Figure 4: Discretization update around the crack tip by local re-triangulation

2.4 Fictitious Crack Model

To model the force transmission over micro crack surfaces where the crack width w is smaller then a critical value

$$0 \leq w \leq w_c, \tag{9}$$

the "Fictitious Crack Model" following Hillerborg et al. 1976 is applied in this study. In this model the normal stresses are formulated depending on the crack width

$$t_n = f_n(w). \tag{10}$$

Based on experimental results this stress-crack-width-relation can be approximated by a bilinear curve following Gustafsson and Hillerborg 1984

$$t_n = \begin{cases} f_{ctm} \cdot \left(1 - 0.85 \dfrac{w}{w_1}\right) & 0 \leq w \leq w_1 \\ 0.15 f_{ctm} \cdot \dfrac{w_c - w}{w_c - w_1} & w_1 \leq w \leq w_c \\ 0 & w > w_c \end{cases} \tag{11}$$

with

$$w_c = \alpha_f \cdot \frac{G_F}{f_{ctm}}, \quad w_1 = 2 \cdot \frac{G_F}{f_{ctm}} - 0.15 w_c, \tag{12}$$

where f_{ctm} is the tensile strength, G_F is the specific energy which is dissipated by the crack opening and α_f is a introduced coefficient. These values are material constants which depend on the concrete properties and can be found in literature for example in the CEB-Modelcode (Telford 1993).
For the numerical implementation of this model the following assumption was done in Häussler-Combe 2001

$$\tilde{t}_n = \begin{cases} c \cdot w & w \leq 0 \\ 2 G_F \dfrac{w}{\tilde{w}_c \cdot w_0} & 0 \leq w \leq w_0 \\ 2 G_F \left(\dfrac{w}{\tilde{w}_c (w_0 - \tilde{w}_c)} - \dfrac{1}{w_0 - \tilde{w}_c} \right) & w_0 \leq w \leq \tilde{w}_c \\ 0 & w > \tilde{w}_c \end{cases} \tag{13}$$

where $\tilde{w}_c$ can be chosen by assuming $\tilde{t}_n^{max} = f_{ctm}$ as $\tilde{w}_c = 2 G_F / f_{ctm}$. The parameter w_0 has no physical meaning and affects the convergence behavior. To avoid the penetration of both crack sides by non-monotonic loading the value of constant c has to be chosen large enough. The approximation curves according to Eq.(11) and Eq.(13) are shown in Fig. 5.
To describe the shear force transmission along the crack surfaces in Häussler-Combe 2001 a simple assumption is recommended which uses the Coulomb friction hypothesis. To activate the friction forces a displacement u_a in crack direction has to be present

$$t_\tau = \begin{cases} \beta \cdot f_n \cdot \dfrac{u}{u_a} & u \leq u_a \\ \beta \cdot f_n & u > u_a \end{cases} \tag{14}$$

To apply the FCM in the presented meshless discretization the transmission of the crack softening forces has to be done between the node pairs of the crack surfaces. To avoid additional external loads at these nodes, linear interface elements are included between the crack surfaces. The used interface elements are usually known as iso-parametric bond elements (Mehlhorn and Kolleger 1995). In both integration points of one element the relative displacements in crack direction and in normal direction are computed by using linear shape functions to calculate the normal and the shear stresses. Numerical investigations on a concrete beam without reinforcement by using the normal stress approximation in Eq.(13) showed force redistributions around the crack, which led to the arising of new cracks next to the first one, caused by the high stiffness values of the interface elements if w is smaller than w_0. This means that this assumption could lead to numerical problems if we compute the displacements implicitly. A better assumption is Eq.(11) where the stiffness gets negative values. To avoid the penetration without introducing a jump in the stress curve we can assume the following relation

$$t_n(w < 0) = t_n^{max} - c \cdot w. \tag{15}$$

By choosing $t_n^{max} = f_{ctm}$ in some cases the implicit iteration could not find equilibrium by monotonic loading with theoretically increasing crack widths, but snapped back into the negative part explained in Eq.(15) where pressure forces are transmitted over the crack surface. In order to avoid this effects the curve was modified as shown in Fig. 6, where the maximum value t_n^{max} was reduced, to obtain numerical stability. The assumed unloading and reloading behavior is displayed additionally in the figure.

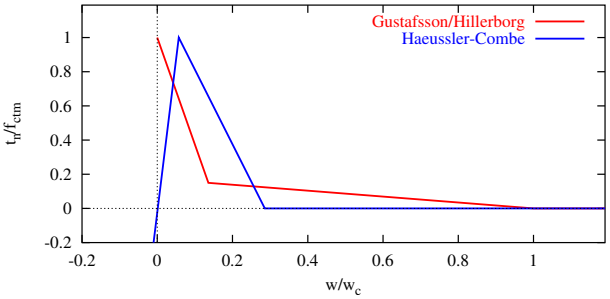

Figure 5: Approximation of the Tension Softening behavior of concrete

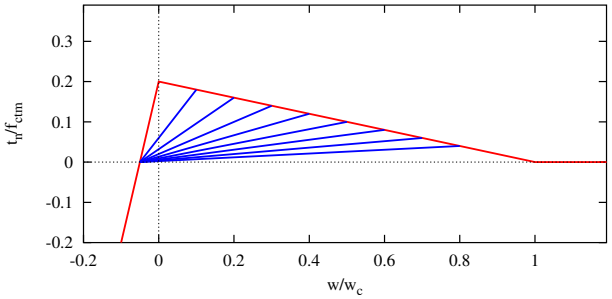

Figure 6: Assumed normal stress function with reloading cycles

2.5 Algorithmic specifics

To apply the presented model in an implicit global Newton-Raphson-Iteration we have to consider some specifics. In order to obtain numerical stability it is necessary to allow only one crack increment per iteration cycle. If the transformation criterion for some finite elements is exceeded, in this iteration cycle no new crack increment should be included to separate the effects by transforming the finite elements and by the force redistribution around a new crack increment. If the theoretical new crack increment touches a finite element, this element has to be transformed first by neglecting the new increment and the iteration cycle has to be repeated.
The included interface elements between the crack nodes need special attention in this form, that after included a new crack increment with belonging interface elements an internal iteration has to take part to obtain an equilibrium between external and internal forces with no nodal restoring forces along the crack surfaces. Then the new global iteration cycle can be done and a new crack increment can arise. If this fact is not considered, a force redistribution around the new crack increment takes part, which leads to the appearance of new cracks and anticipates the development of existing cracks. The internal iteration is comparable with the iteration at the integration point level for nonlinear material

laws, where first the local convergence has to be achieved before a new global iteration cycle can be done. The developed global iteration with included local iteration is shown in Table 1.

- get new external load vector $\mathbf{F}$
- calculate initial deviation between load and global restoring force vector $\Delta\mathbf{F}_0 = \mathbf{R}_F - \mathbf{F}$

- start iteration with iteration count i:

$START$
- get new displacement increment $\Delta\mathbf{u}_i$ by solving $\mathbf{K}_{i-1}\Delta\mathbf{u}_i = \Delta\mathbf{F}_{i-1}$
- merge new displacements $\mathbf{u}_i = \mathbf{u}_{i-1} + \Delta\mathbf{u}_i$ onto the nodes
- build up stress values and check for critical elements
- if no critical elements go to $NO\_TRANSFORM$
- transform critical elements to MLS-components, go to $TRANSFORM$

$NO\_TRANSFORM$
- check for new crack increment
- if found new crack increment without touching a finite element update the discretization and go to $NO\_CRACK\_TRANSFORM$
- do not use new crack increment, but transform touched finite elements

$TRANSFORM$

$NO\_CRACK\_TRANSFORM$
- build up meshless weighting and shape functions
- if new crack increment renumber global degrees of freedom to include the new nodes and to reduce the band width of the stiffness matrix
- build up global load vector $\mathbf{F}$, global restoring force vector $\mathbf{R}_{F_i}$ and stiffness matrix $\mathbf{K}_i$
- calculate the difference norm $NORM = \|\Delta\mathbf{F}_i\|$ of $\Delta\mathbf{F}_i = \mathbf{R}_{F_i} - \mathbf{F}$
- if no new crack increment go to $NO\_INTERNAL\_ITERATION$

- set initial values for the internal iteration: $\Delta\mathbf{F}_{j=0} = \Delta\mathbf{F}_i$, $\mathbf{K}_{j=0} = \mathbf{K}_i$ and $\mathbf{u}_{j=0} = \mathbf{u}_i$
- start internal iteration with iteration count j:

$START\_INTERNAL$
  - get new displacement increment $\Delta\mathbf{u}_j$ by solving $\mathbf{K}_{j-1}\Delta\mathbf{u}_j = \Delta\mathbf{F}_{j-1}$
  - merge new displacements $\mathbf{u}_j = \mathbf{u}_{j-1} + \Delta\mathbf{u}_j$ onto the nodes
  - build up global restoring force vector $\mathbf{R}_{F_j}$ and stiffness matrix $\mathbf{K}_j$
  - calculate the difference norm $NORM\_INTERNAL = \|\Delta\mathbf{F}_j\|$ of $\Delta\mathbf{F}_j = \mathbf{R}_{F_j} - \mathbf{F}$
  - if $NORM\_INTERNAL$ is larger then a given tolerance go back to $START\_INTERNAL$

$END\_INTERNAL$
- set $\Delta\mathbf{F}_i = \Delta\mathbf{F}_j$

$NO\_INTERNAL\_ITERATION$
- if $NORM$ is larger then a given tolerance go back to $START$

END

Table 1: Extended implicit algorithm with included internal iteration

3 Numerical example

By means of this example the influence of the included interface elements on the crack evolution is shown. Therefore a simply supported beam which was tested experimentally by Ebert and Bucher 2002, will be investigated by including the presented elements and without interface elements as done

in Most and Bucher 2003. In Fig.7 the analyzed system with loading and support conditions is shown. The Young's modulus, the tensile strength and the specific crack energy of the concrete are assumed to be lognormally distributed random fields with 0.2 as coefficient of variation and $2.1m$ as correlation length, which corresponds to the beam length. The first 30 eigenvectors are used, which represents the random field which contains 11340 random variables with a quality of 97.70%. The correlation coefficients between different parameters are assumed as $C_{par_{ij}} = 0.8; i \neq j$. The other material properties of the concrete and the properties of the reinforcement are assumed to be deterministic and were taken according to Ebert 2002 and Telford 1993 (Fig.7). The concrete was discretized initially with

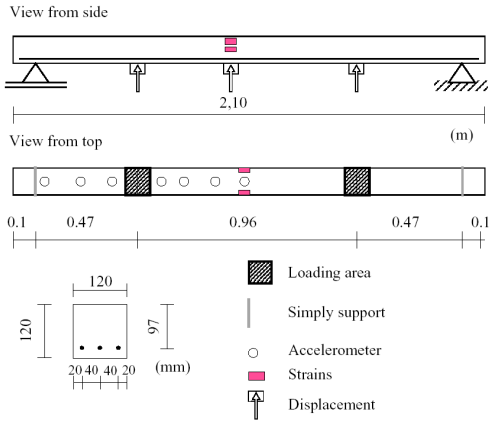

Concrete	Young's modulus	$E = 3.2 \cdot 10^{10} N/m^2$
	Poisson's ratio	$\nu = 0.2$
	Mass density	$\rho = 2700 kg/m^3$
	Tensile strength	$f_{ct} = 3.3 \cdot 10^6 N/m^2$
	Spez. crack energy	$G_F = 85.5 \cdot Nm/m^2$
	FCM parameter	$\alpha_F = 7$
Steel	Young's modulus	$E = 2.1 \cdot 10^{11} N/m^2$
	Poisson's ratio	$\nu = 0.3$
	Mass density	$\rho = 7850 kg/m^3$

Figure 7: Simple supported beam tested in Ebert and Bucher 2002

5x84 9-node-plane elements and the reinforcement with 84 rod elements. The bond behavior between the concrete and the reinforcement was modeled with deterministic bond-link-elements (Mehlhorn and Kolleger 1995) by using a nonlinear law between the shear stress and the relative displacement (Doerr 1980).
In Fig.8 the initial distributions of Young's modulus, tensile strength and specific crack energy of the concrete of one sample are shown. If a new crack increment arises the random field data for tensile strength and specific crack energy of the included interface elements are obtained from the surrounding meshless integration points by using the MLS-approximation in the same manner as for the interpolation of the random field data of new meshless integration points which is described in detail in Most and Bucher 2003. In Fig.9 the longitudinal stresses in the beam are displayed for an external load of 5000 N. The figure shows, that with the included elements the crack evolution stops by about 2/3 of the height which corresponds to the experimental observations. By not using interface elements the crack growth goes further up to 4/5 of the height until the bond between reinforcement and concrete is activated and the tensile force can be transmitted.
To discuss the numerical results, the obtained first natural frequency of the modeled beam is compared with the experimental results. In Fig.10 the relative frequency decrease of the averaged experimental and the numerical results are shown. Above a load of $2.5kN$, at which the crack evolution starts, the numerically and experimentally obtained frequencies decrease. The differences between the two numerical curves show that the considered force transmission and the contact forces in the unloaded state (where the first natural frequency was measured) have an important influence on the dynamic properties. The deviation from the experimental curve is caused by the development of the most cracks in a small load window, which could be an indicator that the crack criterion is not sensitive enough. In further investigations different crack criteria (e.g. based on energy values) and shorter correlation lengths have to be investigated. In general we can summarize, that the improvement of the model by including the presented interface elements lead to a better representation of the observed experimental phenomena.

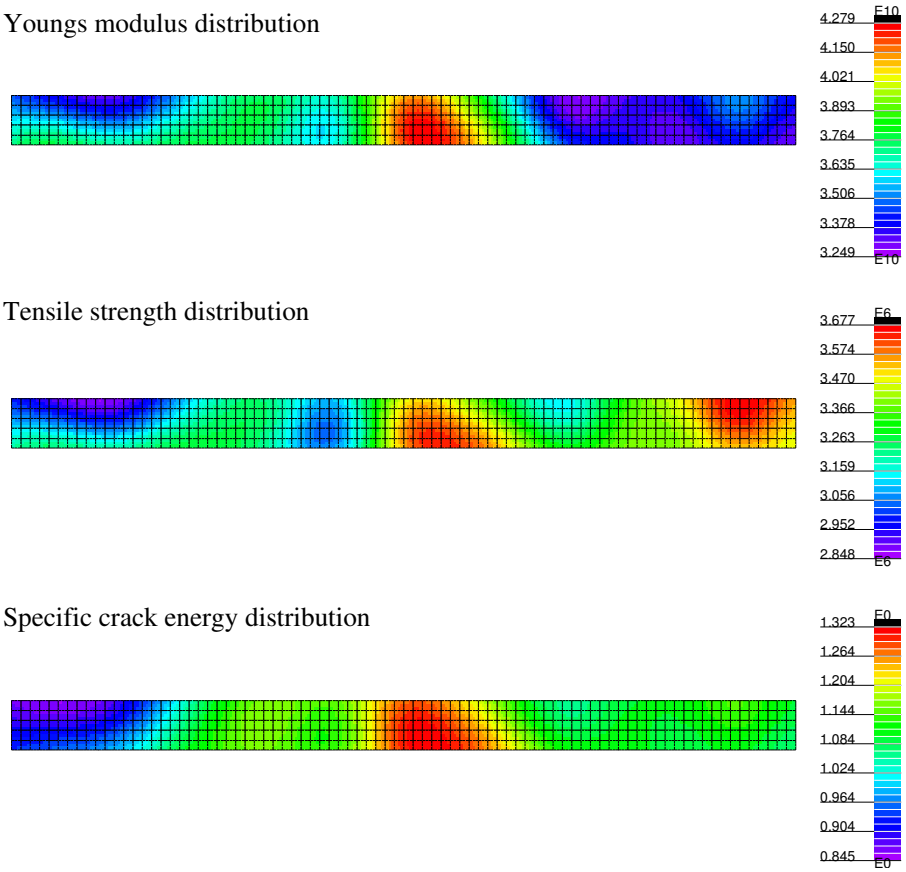

Figure 8: Initial Young's modulus, tensile strength and specific crack energy distribution

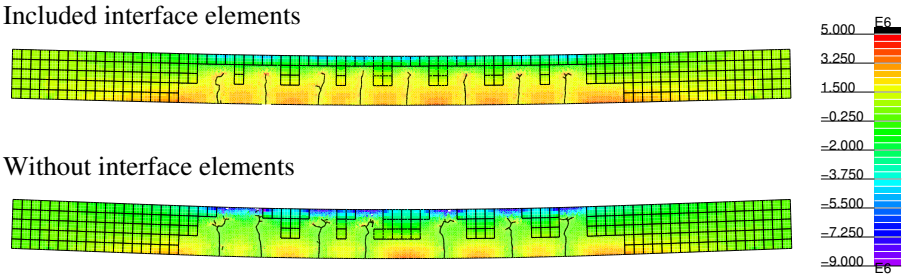

Figure 9: Obtained longitudinal stresses in the beam by using interface elements and without for an external load of 5000 N

4 Conclusion

In this paper a meshless component for stochastic crack simulations is presented. This component internally uses the common MLS-approximation scheme. To enable a direct coupling with finite elements a penalty method is used to enforce the boundary and coupling conditions.
The presented integration scheme by using triangle integration zones is different from usually applied methods and enables the application of an efficient search algorithm by using the triangle neighborhood relations. The material uncertainties of the system are modeled with random fields, which are discretized at the integration points.
The simulation of crack propagation requires an adaptation of the nodes around the crack tip and the transformation of the finite elements to meshless components, where the crack criterion is almost reached. At the moving crack tips a local re-triangulation is sufficient to update the integration zones. To enable the force transmission over the crack surfaces interface elements are placed between the

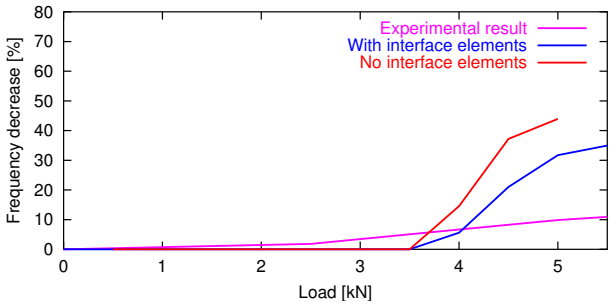

Figure 10: Relative frequency decrease depending of the load values obtained by experimental and numerical investigations

crack nodes, where the assumption in Gustafsson and Hillerborg 1984 was modified to get numerical stability.
On a practical example it was shown that the included elements improve the model by the transmission of the surface forces during monotonic loading and by the representation of the contact forces of closed cracks during reverse loading. This could be shown on the dynamic properties of a simply supported beam under cyclically increasing loading. For future works the authors will investigate different crack criteria for the model in order to reduce the observed effects, that most cracks arise in a small load window, which decreases the numerical stiffness values too fast compared with the experimental results.

Acknowledgment

This research has been supported by the German Research Foundation (DFG) through *Sonderforschungsbereich 524*, which is gratefully acknowledged by the authors.

References

Beissel, S. and T. Belytschko (1996). Nodal integration of the element-free Galerkin method. *Computer Methods in Applied Mechanics and Engineering 139*, 49–74.

Belytschko, T., L. Gu, and Y. Lu (1994). Fracture and crack growth by element-free Galerkin methods. *Modelling and Simulation in Material Scienceand Engineering 2*, 519–534.

Belytschko, T., Y. Krongauz, D. Organ, M. Fleming, and P. Krysl (1996). Meshless methods: an overview and recent developments. *Computer Methods in Applied Mechanics and Engineering 139*, 3–48.

Belytschko, T., Y. Lu, and L. Gu (1994). Element-free Galerkin methods. *International Journal of Numerical Methods in Engineering 37*, 229–256.

Belytschko, T., Y. Lu, and L. Gu (1995a). Crack propagation by element-free Galerkin methods. *Engineering Fracture Mechanics 51*, 295–315.

Belytschko, T., Y. Lu, and L. Gu (1995b). Element-free Galerkin methods for static and dynamic fracture. *International Journal of Solids and Structures 32*, 2547–2570.

Bucher, C. et al. (2002). SLang -*The Structural Language* (5.0 ed.). Bauhaus-University of Weimar, Germany: Institute of Structural Mechanics.

Carpinteri, A., G. Ferro, and G. Ventura (2001). An augmented Lagrangian element-free (ALEF) approach for crack discontinuities. *Computer Methods in Applied Mechanics and Engineering 191*, 941–957.

Cichón, C. and J. Jaśkowiec (1999). Application of Element-free Galerkin Method to crack growth analysis in plain concrete strcutures. In W. Wunderlich (Ed.), *Proc. European. Conf. on Comp. Mechanics, Munich, Germany, August 31 - September 3, 1999*.

Cornelissen, H., D. Hordijk, and H. Reinhardt (1986). Experimental determination of crack softening characteristics of normal and lightweight concrete. *HERON 31*, 45–56.

Doerr, K. (1980). *Ein Beitrag zur Berechnung von Stahlbetonscheiben unter besonderer Berücksichtigung des Verbundverhaltens*. Ph. D. thesis, TH Darmstadt.

Ebert, M. (2002). *Experimentelle und numerische Untersuchung des dynamischen Tragverhaltens von Stahlbetontragwerken unter Berücksichtigung stochastischer Eigenschaften*. Ph. D. thesis, Bauhaus-University Weimar.

Ebert, M. and C. Bucher (2002). Damage effects on the dynamic properties of R/C beams - experimental and numerical investigations. In H. Grundmann and G. Schuëller (Eds.), *Proc. 5th European. Conf. on Structural Dynamics, Munich, Germany, September 2-5, 2002*. Rotterdam: Balkema.

Gross, D. (1996). *Bruchmechanik*. 2nd edition. Berlin/Heidelberg/New York: Springer-Verlag.

Gustafsson, P. and A. Hillerborg (1984). Improvements in concrete design achieved through the application of fracture mechanics. In *Application of Fracture Mechanics to Cementitious Composites. NATO Advanced Research Workshop.*, pp. 639–680. Evanston, USA.

Häussler-Combe, U. (2001). *Elementfreie Galerkin-Verfahren: Grundlagen und Einsatzmöglichkeiten zur Berechnung von Stahlbetontragwerken.* Habilitationthesis, University of Karlsruhe, Germany.

Herrmann, L. (1976). Laplacian-isoparametric grid generation scheme. *J. Eng. Mech. Division, ASCE 102*, 749–756.

Hillerborg, M., M. Modeer, and P. Peterson (1976). Analysis of crack formation and crack growth in concrete by means of fracture mechanics and finite elements. *Cement and Concrete Research 6*, 773–782.

Karutz, H. (2000). *Adaptive Kopplung der Elementfreien Galerkin-Methode mit der Methode der Finiten Elemente bei Rissfortschrittsproblemen*. Ph. D. thesis, Ruhr-Universität Bochum, Germany.

Lancaster, P. and K. Salkauskas (1981). Surface generated by moving least squares methods. *Mathematics of Computation 37*, 141–158.

Mehlhorn, G. and J. Kolleger (1995). Anwendung der Finiten Elemente Methode im Stahlbetonbau. In *Der Ingenieurbau: Grundwissen Bd 6: Rechnerorientierte Baumechanik*. Berlin: Ernst & Sohn.

Moës, N., J. Dolbow, and T. Belytschko (1999). A Finite Element Method for crack growth without remeshing. *International Journal of Numerical Methods in Engineering 46*, 131–150.

Most, T. and C. Bucher (2003). "Moving Least Squares"-elements for stochastic crack propagation simulations coupled with stochastic finite elements. In A. Der Kiureghian, S. Madanat, and J. Pestana (Eds.), *accepted Paper for the ICASP9 2003, San Francisco, Califonia, July 6-9, 2003*. Rotterdam: Balkema.

Peraire, J., M. Vahdati, K. Morgan, and O. Zienkiewicz (1987). Adaptive remeshing for compressible flow computations. *J. Comp. Phys. 72*, 449–466.

Telford, T. (1993). *CEB-FIP Modelcode 1990*. London.